SELECTED HEAVY FLAVOR RESULTS FROM THE TEVATRON*

Jianming Qian

On behalf of the CDF and the DØ Collaborations

Department of Physics, University of Michigan
Ann Arbor, MI 48109, USA

(Received November 15, 2006)

The large datasets provided by the Tevatron $p\bar{p}$ collider have offered CDF and DØ experiments unprecedented opportunities to measure B hadron masses, lifetimes, and decay branching fractions with great precision, reconstruct and identify resonances that have never been observed before, and set stringent limits on many rare decays. In this paper, I summarize some of the recent heavy flavor results from the Tevatron.

PACS numbers: 12.15.Ff, 13.20.He, 13.20.Jf, 13.25.Hw

1. Introduction

The Tevatron proton and anti-proton collider has been running exceedingly well. It has achieved a record instantaneous luminosity of 1.7×10^{32} cm^{-2}s^{-1} and delivered over 1.6 fb^{-1} to both the CDF and DØ experiments at a center-of-mass energy of 1.96 TeV so far in Run II. Both experiments have accumulated datasets of more than 1 fb^{-1}. Datasets of this size offer unique opportunities not just for high p_{T} physics, but also for B physics. Both CDF and DØ have rich B physics programs. A large number of B physics results from Tevatron Run II have been either published or presented at conferences. I cannot possibly cover all the results in my short talk. Instead, I will summarize a few selected topics falling roughly into three areas: spectroscopy, rare decays and B_s^0 physics. People interested in details or in results not covered in this paper are encouraged to visit the CDF and DØ B physics web pages [1].

Bottom quarks are copiously produced in $p\bar{p}$ collisions at the Tevatron. The cross section is estimated to be ~ 100 μb. At a typical instantaneous luminosity of 1×10^{32} cm^{-2} s^{-1}, this cross section gives a rate of 10 kHz of

* Presented at the "Physics at LHC" Conference, Kraków, Poland, July 3–8, 2006.

real b-quarks. Like other quarks, b-quarks are promptly hadronized to form B hadrons. Unlike the e^+e^- B factories at SLAC and KEK, where only lightest B hadrons are formed, a large variety of B hadrons are produced at the Tevatron. The expected compositions are $\sim 80\%$ B^+ and B^0, $\sim 10\%$ each for B_s meson and B-baryons. Other B hadrons are also produced, but at small rates. For example, it is expected that 0.05% of all B hadrons are B_c mesons. Events with real B's are buried under even larger QCD backgrounds (with a total inelastic cross section of 60 mb!). Triggering B events is a real challenge. In CDF, B hadrons are triggered either by muons from B decays (semileptonic or J/ψ) or by their long decay distances. In DØ, the trigger relies solely on muons from B decays.

2. Masses, lifetimes and branching ratios

2.1. B_c^+ mass

The B_c^+ meson[1] is a $\bar{b}c$ bound state formed by two heavy quarks: a bottom antiquark and a charm quark. It provides a unique opportunity to test heavy-quark effective theory that has been successful in describing both lighter charm and bottom hadrons.

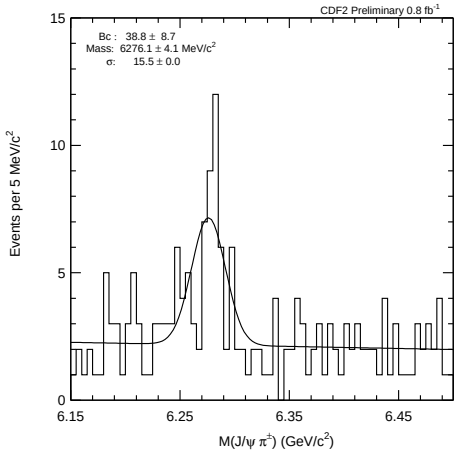

Fig. 1. The CDF reconstructed $J/\psi\pi^+$ invariant mass distribution with a binned fit superimposed.

The B_c^+ meson is not produced at SLAC and KEK B factories and is rarely produced at the Tevatron. Therefore its mass is not well known. Lattice QCD calculation predicts a mass of $6304 \pm 12^{+18}_{-0}$ MeV$/c^2$ [4]. The CDF experiment has fully reconstructed the B_c^+ meson through its decay $B_c^+ \to J/\psi\pi^+$ with the subsequent $J/\psi \to \mu^+\mu^-$ decay. Fig. 1 shows the

[1] Charge conjugation is implied throughout this proceeding.

reconstructed $J/\psi\pi^+$ mass distribution from a sample of 800 pb^{-1}. A fit to signal and background contributions yields 39 B_c^+ candidates, corresponding to over 6 standard deviations for a false signal from a potential background fluctuation. The B_c^+ mass is measured to be $6275.2 \pm 4.3(\text{stat}) \pm 2.3(\text{syst})$ MeV$/c^2$, in good agreement with the lattice calculation. This is the most precise B_c^+ mass measurement to date.

2.2. Λ_b lifetime

The lifetime of all B hadrons are expected to be equal based on a simple quark-spectator model. However, when non-spectator effects are taken into account, they give rise to a lifetime hierarchy of $\tau(B^+) \geq \tau(B^0) \approx \tau(B_s^0) > \tau(\Lambda_b) \gg \tau(B_c^+)$ [5]. Precision measurements of B hadron lifetimes are important to test theory predictions. CDF has reported a new measurement of Λ_b (a udb baryon) lifetime in its decay channel $\Lambda_b \to J/\psi(\mu^+\mu^-)\,\Lambda(p\pi^-)$. Analyzing 1 fb^{-1} of data, 538 ± 38 Λ_b candidates are reconstructed. Their measured proper decay length distribution is shown in Fig. 2(left). A fit to the distribution results in a lifetime of $1.593^{+0.083}_{-0.078}(\text{stat}) \pm 0.033(\text{syst})$ ps. This measurement is compared with previous measurements in Fig. 2 (right). It is interesting to note that the new measurement is significantly above the world average of all previous measurements, but is closer to those of B mesons.

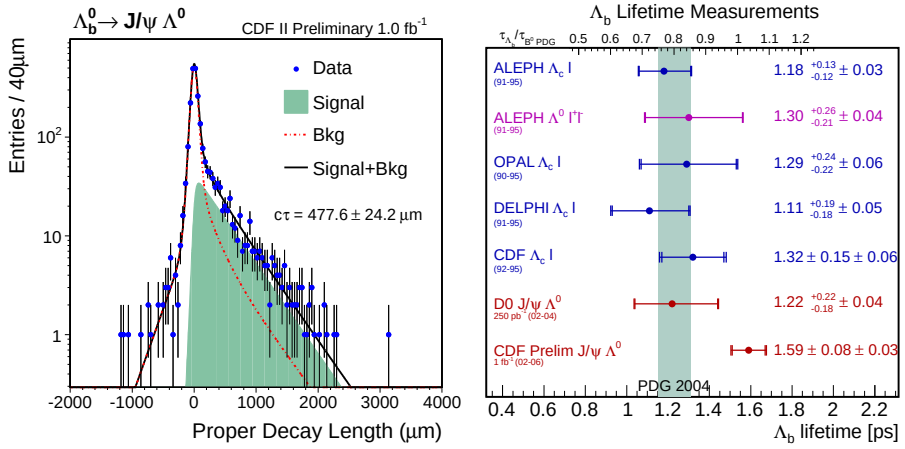

Fig. 2. CDF: The proper decay length distribution of the $\Lambda_b \to J/\psi\Lambda$ candidates superimposed with fitting results (left) and a comparison of this result with previous measurements (right).

2.3. Branching fractions of $B_s^0 \to D_s^{+(*)} D_s^{-(*)}$

As discussed in Section 4, the $B_s^0 - \bar{B}_s^0$ mixing can produce a large width difference $\Delta\Gamma_s$ between the two B_s mass eigenstates. The branching fraction of the $B_s^0 \to D_s^{+(*)} D_s^{-(*)}$ decays is directly proportional to $\Delta\Gamma_s$. Thus measurement of this branching ratio allows for the determination of $\Delta\Gamma_s$. Both CDF and DØ have recently reported results on this topic.

CDF fully reconstructs the $B_s^0 \to D_s^+ D_s^-$ decay through the identification of $D_s^\pm$ in its subsequent $D_s \to \phi(K^+K^-)\pi, KK^*(K\pi), \pi\pi\pi$ decay. In a data sample of 355 pb^{-1}, a total 23.5 ± 5.5 candidates are identified. Fig. 3 shows the reconstructed $D_s^+ D_s^-$ mass distribution in the $D_s^+ \to \phi\pi^+$ decay. This represents the first observation of this fully reconstructed B_s^0 decay mode. The measured ratio of branching fractions is

$$\frac{\mathrm{Br}(B_s^0 \to D_s^+ D_s^-)}{\mathrm{Br}(B_D^0 \to D_s^+ D^-)} =$$
$$1.67 \pm 0.41(\mathrm{stat}) \pm 0.12(\mathrm{syst}) \pm 0.24(f_s/f_d) \pm 0.38(\mathrm{Br}D_s \to \phi\pi)\,.$$

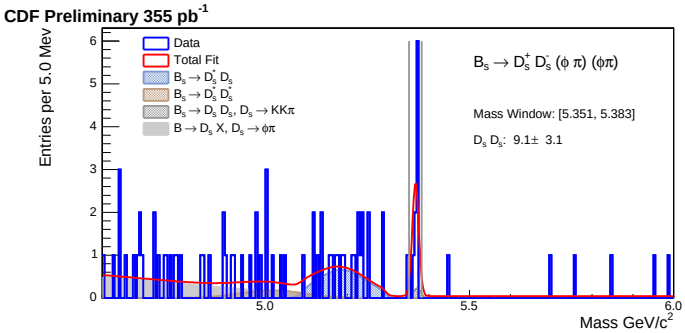

Fig. 3. The CDF invariant mass distribution of $D_s^+ D_s^-$ candidates with D_s^+ reconstructed from its decay to $\phi\pi^+$.

The DØ analysis partially reconstructs $B_s^0 \to D_s^{+(*)} D_s^{-(*)} \to D_s^+ D_s^- + X \to (\phi\pi^+)(\phi\mu^-\bar{\nu}) + X$ decay. Thus the final state includes $D_s^+ D_s^-$, $D_s^{+*} D_s^-$, $D_s^{+*} D_s^{-*}$. The photons and π^0's from $D_s^{+*} \to D_s^+\gamma, D_s^+\pi^0$ decays are not reconstructed. The analysis searches for an additional ϕ in an event with a muon and an identified $D_s^+ \to \phi(K^+K^-)\pi^+$ candidate. The measured yield 19.3 ± 7.8 is then normalized to that of $B_s^0 \to D_s^{+(*)}\mu^-\bar{\nu}$ decay. Using Particle Data Group [6] values of $\mathrm{Br}(D_s^+ \to \phi\mu^+\nu)$ and $\mathrm{Br}(B_s^0 \to D_s^{-(*)}\mu^+\nu)$, the branching fraction of $B_s^0 \to D_s^{+(*)} D_s^{-(*)}$ is measured to be $0.071 \pm 0.032(\mathrm{stat})^{+0.029}_{-0.025}(\mathrm{syst})$.

2.4. Excited B mesons

Apart from the well established $L = 0$ S-states ($B_d^0, B^+, B_s^0, \dots$), the quark model predicts the existence of two wide (B_0^* and B_1^*) and two narrow (B_1 and B_2^*) bound ($\bar{b}d$) $L = 1$ P-states, collectively called B^{**} states. After nearly 30 years of the b quark discovery, little is known about these states experimentally. However, these states are expected to be produced at the Tevatron. The wide states decay through the S-wave and therefore have a large width of $\mathcal{O}(100)$ MeV. The resonances of such states are too broad to be identified. On the other hand, the two narrow states decay through the D-wave and are expected to have a small width of $\mathcal{O}(10)$ MeV. B_1 and B_2^* are expected to have decay modes $B_1 \to B^{+*}\pi^-$, $B_2^* \to B^{+*}\pi^-$, $B_2^* \to B^+\pi^-$ with $B^{+*} \to B^+\gamma$. The soft photon from the B^{+*} decay is not reconstructed. Both the CDF and DØ experiments have reported observations of these narrow states. Both analyses began with the reconstruction of the B^+ meson in its $J/\psi(\mu^+\mu^-)K^+$ (CDF and DØ) and $\bar{D}^0(K^+\pi^-)\pi^+$ (CDF) decay modes. The identified B^+ meson is then combined with a track consistent with originating from the same primary vertex to form B_1 and B_2^* candidates. Fig. 4 (left) shows the CDF invariant mass distribution of $B^+\pi^-$ combinations. Fits to these distributions resulted $M(B_1) = 5734 \pm 3 \pm 2$ MeV/c^2, $M(B_2^*) = 5738 \pm 5 \pm 1$ MeV/c^2 for CDF and $M(B_1) = 5720.8 \pm 2.5 \pm 5.3$ MeV/c^2, $M(B_2^*) - M(B_1) = 25.2 \pm 3.0 \pm 1.1$ MeV/c^2, $\Gamma(B_2^*) \equiv \Gamma(B_1) = 6.6 \pm 5.3 \pm 4.2$ MeV for DØ. These results are consistent with each other and represent the first observations of B_1 and B_2^* excited mesons.

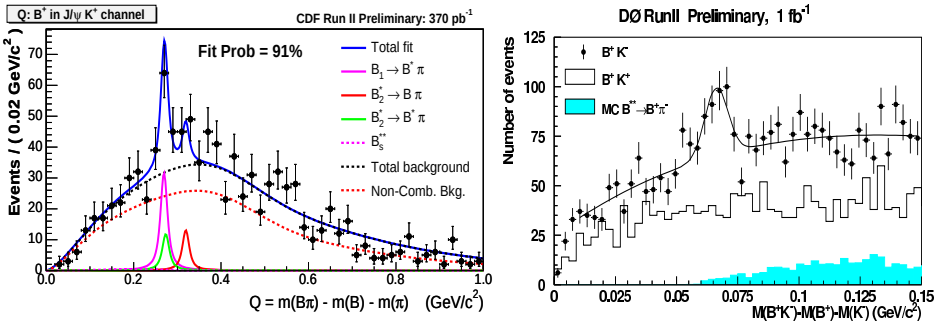

Fig. 4. The CDF mass difference $M(B^+\pi^-) - M(B^+) - M(\pi^-)$ (left) and the DØ mass difference $M(B^+K^-) - M(B^+) - M(K^-)$ (right). Curves represent fits to signal and background contributions.

Similar to the $\bar{b}d$ system, the quark model also predicts 4 P-states for the $\bar{b}s$ system. DØ has searched for the B_{s2}^* state, a counterpart of the B_2^* state, through its decay $B_{s2}^* \to B^+K^-$ with $B^+ \to J/\psi(\mu^+\mu^-)K^+$. The B^+K^- invariant mass distribution from a sample of 1 fb^{-1} is shown in Fig. 4 (right).

The B^*_{s2} signal is evident. A fit yields 135 ± 31 B^*_{s2} candidates with mass $M(B^*_{s2}) = 5839.1 \pm 1.4 \pm 1.5$ MeV/c^2. This is the first observation of the B^*_{s2} meson.

3. Rare decays

Flavor changing neutral current (FCNC) decays are forbidden at tree level in the standard model (SM) and can proceed via higher order penguin or box diagrams. Many extensions of the SM allow for tree level diagrams or alternative loop diagrams for FCNC that could significantly alter the decay rate with respect to SM expectations.

3.1. $B^0_d, B^0_s \to \mu^+\mu^-$

In the SM, the branching fraction for $B^0_s \to \mu^+\mu^-$ is expected to be $(3.42 \pm 0.54) \times 10^{-9}$ [7]. The branching fraction of $B_d \to \mu^+\mu^-$ decay is further suppressed by CKM matrix elements $|V_{td}/V_{ts}|^2$ leading to a SM prediction $(1.00 \pm 0.14) \times 10^{-10}$. An observation of these decays at the Tevatron would signal new physics beyond the standard model [8]. Both CDF and DØ have published limits on these decays. Here, I will discuss the latest result from CDF.

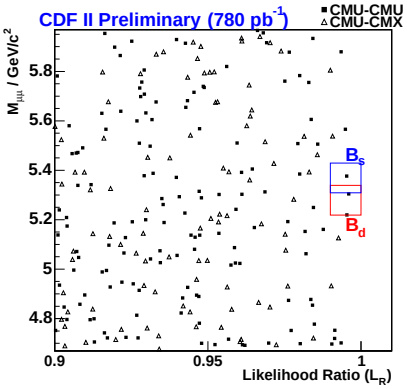

Fig. 5. The CDF invariant mass distribution versus the event likelihood ratio (signal/background). Boxes indicate expected regions for $B^0_d, B^0_s \to \mu^+\mu^-$ decays.

The search for $B^0_d, B^0_s \to \mu^+\mu^-$ involves looking for an excess in the $\mu^+\mu^-$ invariant mass spectrum consistent with the B^0_d or B^0_s masses. The challenge is to reduce backgrounds from Drell–Yan processes, semileptonic decays of bottom and charm hadrons, and instrumental sources. To this end, event kinematics such as $\mu^+\mu^-$ decay length, isolation, and pointing angles are explored. CDF constructed likelihoods for signal and background events and cut on the likelihood ratio to reduce backgrounds. The observed dimuon mass *versus* the likelihood ratio distribution from a sample

of 720 pb^{-1} is displayed in Fig. 5. Three candidate events are observed in the expected signal region, consistent with contributions from background processes. CDF therefore sets limits $\mathrm{Br}(B_d^0 \to \mu^+\mu^-) < 3.0 \times 10^{-8}$ and $\mathrm{Br}(^0\!\to \mu^+\mu^-) < 1.0 \times 10^{-7}$, both at 95% confidence level (CL). The limit on B_s^0 is only a factor of 50 above the standard model expectation.

3.2. $B_s^0 \to \mu^+\mu^-\phi$

The decay $B_s^0 \to \mu^+\mu^-\phi$ is an exclusive FCNC decay corresponding to the $b \to s\ell^+\ell^-$ transition at quark level. Within the SM the decay rate $B_s^0 \to \mu^+\mu^-\phi$ is predicted to be about 1.6×10^{-6} [9] excluding long-distance effects from charmonium resonances. The uncertainty on the rate is large, estimated to be up to 30% due to poorly known form factors. In the two-Higgs doublet model, the rate might be enhanced [10].

DØ has searched for the $B_s^0 \to \mu^+\mu^-\phi$ decay using techniques similar to those employed for $B_d^0, B_s^0 \to \mu^+\mu^-$ analyses. The ϕ meson is reconstructed through its decay to K^+K^-. The $\mu^+\mu^-$ pair consistent with J/ψ or ψ' decay is removed. Fig. 6 shows the $\mu^+\mu^-\phi$ mass distribution after all selection requirements obtained from a sample of about 300 pb^{-1}. No event is observed in the signal region. A limit of $\mathrm{Br}(B_s^0 \to \mu^+\mu^-\phi) < 4.1 \times 10^{-6}$ at 95% CL is obtained. This limit is only a factor of 3 above the expected SM value.

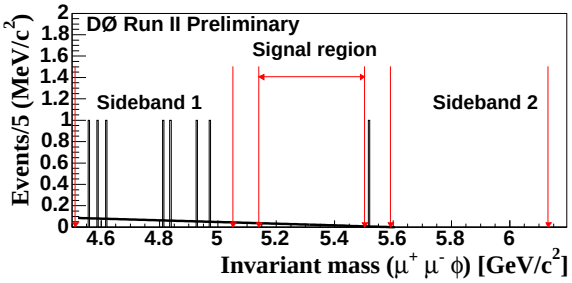

Fig. 6. The DØ $\mu^+\mu^-\phi$ mass distribution after all selection cut.

3.3. $D^+ \to \mu^+\mu^-\pi^+$

Unlike down-type quarks, the FCNC processes involving up-type quarks are less explored experimentally. There are several scenarios of new phenomena [11] that predict deviations from the SM in the up sector. In the SM, the inclusive rate for $D^+ \to \mu^+\mu^-\pi^+$ is expected to be dominated by long distance contributions with $\mu^+\mu^-$ from intermediate resonances such as ϕ and ω. DØ has searched for the $D^+ \to \mu^+\mu^-\pi^+$ decay with the $\mu^+\mu^-$ pair from both the resonances and the continuum.

Fig. 7 shows the invariant $\mu^+\mu^-\pi^+$ mass distribution, requiring $\mu^+\mu^-$ to be from the ϕ mass window $0.96 \leq m_{\mu\mu} \leq 1.06$ GeV/c^2. A fit to the observed distribution with $D^+ \to \phi\pi^+$, $D_s^+ \to \phi\pi^+$, and background contributions yield 25±9 D^+ candidates. Normalizing to the rate of D_s^+, DØ has measured $\mathrm{Br}(D^+ \to \phi\pi^+ \to \mu^+\mu^-\pi^+) = (1.75 \pm 0.70 \pm 0.50) \times 10^{-6}$, a significant improvement over the previous measurement by CLEO [12]. Requiring $\mu^+\mu^-$ to be from the continuum *i.e.* $m_{\mu\mu} \leq 0.96$ GeV/c^2 or $m_{\mu\mu} \geq 1.06$ GeV/c^2, 17 D^+ candidate events are observed with an estimated 20.9 ± 3.4 events from backgrounds. Without excess, DØ sets a limit $\mathrm{Br}(D^+ \to \mu^+\mu^-\pi^+) < 4.7 \times 10^{-6}$ at 90% CL.

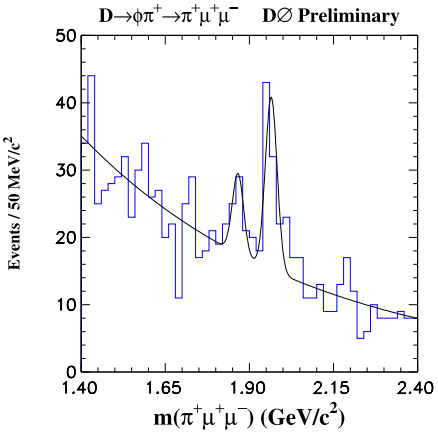

Fig. 7. The DØ $\mu^+\mu^-\pi^+$ mass distribution requiring $0.96 < m_{\mu\mu} < 1.06$ GeV/c^2. The two peaks are expected from D^+ (left) and D_s^+ (right) contributions.

4. B_s^0 Physics

Similar to the $B_d^0 - \bar{B}_d^0$ system, the $B_s^0 - \bar{B}_s^0$ system is expected to mix and oscillate, as a result of the weak interaction involving box diagrams. The mixing leads to two mass eigenstates with different values of mass and decay width. In the SM, the heavier and lighter mass eigenstates are largely CP-even and CP-odd states, respectively. As $B_s^0 - \bar{B}_s^0$ oscillates, the relative mixture of CP-even and CP-odd states changes. Since the two CP states are expected to decay with different angular distributions, the mixture at decay can be determined by studying angular distributions of a decay mode common to both B_s^0 and $\bar{B}_s^0$ such as $B_s^0, \bar{B}_s^0 \to J/\psi\,\phi$. Denoting the mass difference $\Delta m_s = M_{\mathrm{H}} - M_{\mathrm{L}}$, the width difference $\Delta\Gamma_s = \Gamma_{\mathrm{L}} - \Gamma_{\mathrm{H}}$, and the average width $\Gamma_s = (\Gamma_{\mathrm{L}} + \Gamma_{\mathrm{H}})/2$, the time dependent probability that an initial B_s^0 meson decays at time t as a $\bar{B}_s^0$ (or *vice versa*) is given by $P^{\mathrm{osc.}}(t) = \Gamma_s e^{-\Gamma_s t}(1 - \cos\Delta m_s t)/2$, assuming that $\Delta\Gamma_s/\Gamma_s$ is small. Therefore, Δm_s

can be determined from the oscillation measurement while the separation of the two CP components in $J/\psi\,\phi$ decay allows the measurement of the lifetime difference $\Delta\Gamma_s$.

4.1. B_s^0 lifetime difference

There have been considerable interests in the $\Delta\Gamma_s$ results [14] from the Tevatron over the last couple of years. CDF reported the first direct measurement of $\Delta\Gamma_s$ in 2004 with a number unexpectedly large. DØ subsequently reported their first measurement that is in good agreement with the expectation.

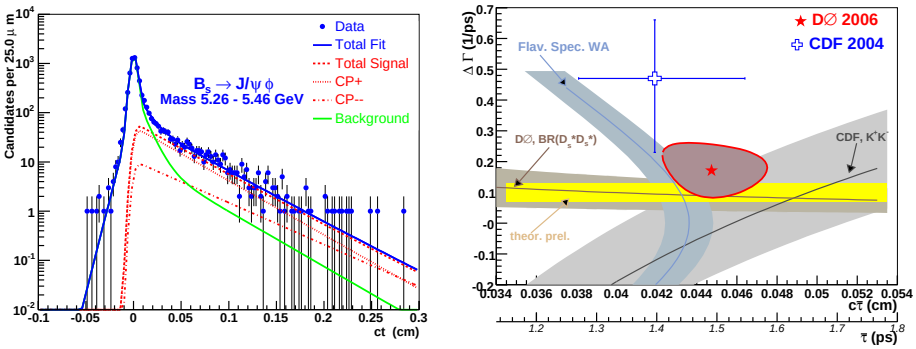

Fig. 8. The DØ proper decay length of $B_s^0, \bar{B}_s^0 \to J/\psi\,\phi$ candidates (left) and the DØ one — σ (stat) contour in the plane of $\Delta\Gamma_s$ *versus* $c\bar{\tau}$ (right).

DØ has recently updated its measurement with 800 pb^{-1}. The kinematics of $B_s^0, \bar{B}_s^0 \to J/\psi(\mu^+\mu^-)\phi(K^+K^-)$ decay can be characterized by three angles [13]. The lifetime difference and the average lifetime can be extracted through a simultaneous fit to distributions of the three decay angles and the proper decay length. Fig. 8 (left) shows the measured decay length distribution. Also shown in the figure are contributions from CP-even and CP-odd states determined from the fit. The average lifetime and decay width difference are determined from a simultaneous fit to these distributions:

$$\bar{\tau}_{B_s^0} = \frac{\tau_{\rm H} + \tau_{\rm L}}{2} = 1.53 \pm 0.08^{+0.01}_{-0.03}\ {\rm ps}\,,$$

$$\Delta\Gamma_s = \Gamma_{\rm L} - \Gamma_{\rm H} = 0.15 \pm 0.10^{+0.03}_{-0.04}\ {\rm ps}^{-1}\,.$$

Fig. 8 (right) compares the Tevatron results with the theoretical expectation and other flavor or CP specific measurements.

4.2. B_s^0–$\bar{B}_s^0$ oscillation

Both DØ and CDF have reported results of B_s^0–$\bar{B}_s^0$ oscillation frequency [15]. These analyses are briefly described below. There are three key components for studying B_s^0–$\bar{B}_s^0$ oscillation: flavor tagging at the production, flavor determination at the decay and measurement of the proper decay time. In the DØ analysis, the flavor at the production is tagged from the electron or muon charge of the semileptonic decay and jet charge of the other B hadron (opposite-side tagging). The tag gives a tagging power $\epsilon\mathcal{D}^2 \sim 2.5\%$. The flavor at the decay is determined through the partial reconstruction of semileptonic $B_s^0 \to D_s^- \mu^+ \nu$ decays with $D_s^- \to \phi(K^+K^-)\pi^-$. The reconstructed decay vertex, corrected for Lorentz boost, gives the proper decay length. The typical resolution for the proper decay length is about 150 fs. Analyzing 1 fb^{-1}, DØ reconstructs about 5,600 $B_s^0 \to \mu^+ \nu D_s^-$ decays with opposite-side flavor tagging. An unbinned likelihood fit using decay time and its resolution, flavors at production and decay is employed to extract the oscillation frequency.

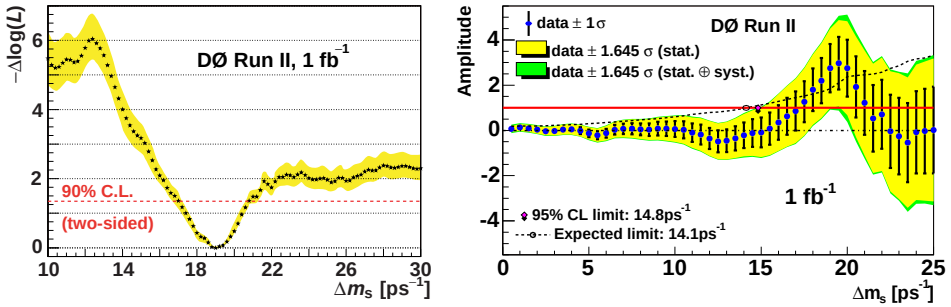

Fig. 9. The DØ value of $-\Delta \log \mathcal{L}$ (left) and B_s^0 oscillation amplitude (right) as functions of oscillation frequency Δm_s.

Fig. 9 (left) shows the value of $-\Delta \log \mathcal{L}$ of the fit as a function of Δm_s, indicating a favored value of 19 ps^{-1} with a range of $17 < \Delta m_s < 21$ ps^{-1} at the 90% CL, the first direct two-sided limit on the oscillation frequency. The result of an amplitude scan [16] is shown in Fig. 9 (right). In this method, oscillation and non-oscillation are characterized by amplitude $\mathcal{A} = 1$ and $\mathcal{A} = 0$ respectively. At $\Delta m_s = 19$ ps^{-1} the measured data point deviates from the hypothesis of no oscillation ($\mathcal{A} = 0$) by 2.5 standard deviations.

CDF employs both opposite-side ($\epsilon\mathcal{D}^2 \sim 1.5\%$) and same-side ($\epsilon\mathcal{D}^2 \sim$ 3.5–4.0%) tagging to determine the flavor at the production. The same-side tagging assumes that when a B_s^0 (or $\bar{B}_s^0$) meson is formed through hadronization, a corresponding Kaon is produced. By measuring the charge of the Kaon at the same-side of the decaying $B_s^0(\bar{B}_s^0)$ meson, the flavor

at the production is determined. Apart from the partial $B_s^0 \to D_s^- \mu^+ \nu$ reconstruction as DØ discussed above, CDF also fully reconstructs hadronic $B_s^0 \to D_s^-(3)\pi^+$ decays thanks to their secondary vertex trigger capability. Without missing neutrinos, the hadronic reconstruction gives superior decay length resolution, estimated to be around 90 fs. In total, CDF reconstructs 37,000 B_s^0 ($\bar{B}_s^0$) in the semileptonic mode and 3,600 in the hadronic mode. Fig. 10 (left) shows the invariant mass distribution of $D_s^-\pi^+$ with $D_s^- \to \phi(K^+K^-)\pi^-$.

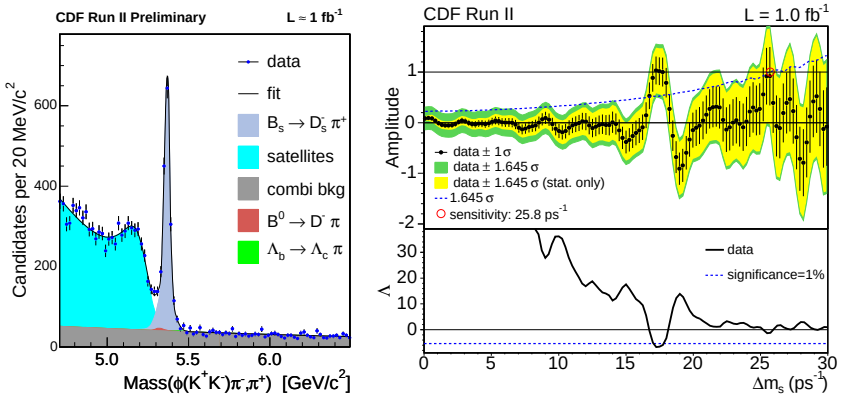

Fig. 10. CDF: The $D_s^-(\phi\pi^-)\pi^+$ invariant mass distribution (left) and the measured amplitude values and uncertainties (upper) and the logarithm of the likelihood ratio (lower) *versus* oscillation frequency Δm_s (right).

The fitted value of the amplitude as a function of the oscillation frequency is shown in Fig. 10 (right, upper plot). At $\Delta m_s = 17.3$ ps^{-1}, the observed amplitude $\mathcal{A} = 1.03 \pm 0.28(\text{stat})$ is consistent with unity, indicating that the data are compatible with $B_s^0 - \bar{B}_s^0$ oscillation with that frequency, while the amplitude is inconsistent with zero at 3.7 standard deviations. The significance of the potential signal is evaluated using the logarithmic likelihood ratio Λ of $\mathcal{A} = 0$ and $\mathcal{A} = 1$: $\Lambda = \log[\mathcal{L}^{\mathcal{A}=0}/\mathcal{L}^{\mathcal{A}=1}]$. The lower plot of Fig. 10 (right) shows Λ as a function of Δm_s. Under the hypothesis that the signal is due to the oscillation, the frequency is measured to be $\Delta m_s = 17.31^{+0.33}_{-0.18}(\text{stat}) \pm 0.07(\text{syst})$ ps^{-1}. This is the first measurement of $B_s^0 - \bar{B}_s^0$ oscillation frequency.

5. Summary

Selected latest heavy flavor results covering spectroscopy, rare decays and B_s^0 mixing and oscillation from the CDF and DØ experiments are summarized in this talk. On the spectroscopy, topics covered are B_c^+ mass and Λ_b lifetime measurements from CDF, branching fractions of $B_s^0 \to D_s^{+(*)} D_s^{-(*)}$

determinations from both CDF and DØ, and observations of excited B^{**} mesons from CDF and DØ. In the area of rare decays, recent results on FCNC processes $B_d^0, B_s^0 \to \mu^+\mu^-$ (CDF), $B_s^0 \to \mu^+\mu^-\phi$ (DØ) and $D^+ \to \mu^+\mu^-\pi^+$ (DØ) are presented. On B_s^0 mixing and oscillation, the latest results on the lifetime difference (DØ) and $B_s^0 - \bar{B}_s^0$ oscillation (DØ and CDF) are presented.

It is truly a pleasure to present many exciting B physics results from the Tevatron. I thank my colleagues at the Tevatron for their tireless and dedicated effort and apologize to them for leaving out many interesting results. I am grateful to B physics group conveners of both CDF and DØ (Guennadi Borissov, Brendan Casey, Matthew Herndon, Kevin Pitts) for their support. I wish to express my gratitude to the conference organizers for their hospitality and successful hosting of the conference.

REFERENCES

[1] CDF B physics: `www-cdf.fnal.gov/physics/new/bottom/bottom.html`; DØ B Physics: `www-d0.fnal.gov/Run2Physics/WWW/results/b.htm`
[2] CDF Collaboration, D. Acosta *et al.*, *Phys. Rev.* **D71**, 032001 (2005).
[3] DØ Collaboration, V.M. Abazov *et al.*, "The Upgraded DØ Detector" submitted to *Nucl. Instrum. Methods Phys. Res. A*, Fermilab-Pub-05/341-E `[physics/0507191]`.
[4] I.F. Allison *et al.*, *Phys. Rev. Lett.* **94**, 172001 (2005).
[5] I.I.Y. Bigi, `hep-ph/0001003`.
[6] S. Eidelman *et al.*, *Phys. Lett. B* **592**, 1 (2004).
[7] A.J. Buras, *Phys. Lett. B* **566**, 115 (2003).
[8] S. Choudhury, N. Gaur, *Phys. Lett. B* **451**, 86 (1999); K.S. Babu, C. Kolda, *Phys. Rev. Lett.* **84**, 228 (2000); R. Dermisek *et al.*, *J. High Energy Phys.* **04**, 037 (2003); D. Auto *et al.*, *J. High Energy Phys.* **06**, 023 (2003); T. Blazek *et al.*, *Phys. Lett. B* **589**, 39 (2004); R. Arnowitt *et al.*, *Phys. Lett. B* **538**, 121 (2002).
[9] C.Q. Geng, C.C. Liu, *J. Phys.* **G29**, 1103 (2003) `[hep-ph/0303246]`.
[10] G. Erkol, G. Turan, *Eur. Phys. J.* **C25**, 575 (2002) `[hep-ph/0203038]`.
[11] K. Agashe, M. Graesser, *Phys. Rev.* **D54**, 4445 (1996); S. Fajfer, S. Perlovsek, *Phys. Rev.* **D73**, 054026 (2006).
[12] CLEO Collaboration, Q. He *et al.*, *Phys. Rev. Lett.* **95**, 221802 (2005).
[13] I. Dunietz, R. Fleischer, U. Nierste, *Phys. Rev.* **D63**, 114015 (2001).
[14] CDF Collaboration, D. Acosta *et al.*, *Phys. Rev. Lett.* **94**, 101803 (2005); DØ Collaboration, V.M. Abazov *et al.*, Phys. Rev. Lett. **95**, 171801 (2005).
[15] DØ Collaboration, V.M. Abazov *et al.*, *Phys. Rev. Lett.* **97**, 021802 (2006); CDF Collaboration, A. Abulencia *et al.*, `hep-ex/0606027`.
[16] H.G. Moser, A. Roussarie, *Nucl. Instr. Meth.* **A384**, 491 (1997).